EurJOC
European Journal of Organic Chemistry

A Journal of
ChemPubSoc Europe

Accepted Article

Title: Blue-fluorescent probes for lipid droplets based on dihydrochromeno- pyrazolepyridine and pyrrolopyridine

Authors: Martin Becerra-Ruiz, Victor Vargas, Patricio Gregorio Jara, Cristian Tirapegui, Carlos Carrasco, Marco Tulio Núñez, Nicolas Lezana, Antonio Galdámez, and Marcelo Vilches Herrera

To be cited as: *Eur. J. Org. Chem.* 10.1002/ejoc.201701633

Link to VoR: http://dx.doi.org/10.1002/ejoc.201701633

Supported by
ACES Asian Chemical Editorial Society

WILEY-VCH

10.1002/ejoc.201701633
WILEY-VCH

Blue-fluorescent probes for lipid droplets based on pyrazolepyridine or pyrrolopyridine fused dihydrochromeno

Martín Becerra-Ruiz,[a] Victor Vargas,[a] Patricio Jara,[a] Cristian Tirapegui,[c] Carlos Carrasco,[b]+ Marco Nuñez,[b]+ Nicolás Lezana, [a] Antonio Galdámez,[a] and Marcelo Vilches-Herrera.[a]*

Abstract: Lipid droplets (LDs) have been recognized as highly dynamic cellular organelles involved in important biological functions for the survival of organisms such as supplying food or energy. Nevertheless, lipid storage must be tightly controlled, since both its excess and the inability to store lipids can be detrimental to the organism, resulting in metabolic diseases or multifaceted systemic problems. Visualization and monitoring the concentration of LDs is essential to understand these processes. Commercially available LD dyes such as nile red and BODIPY offer several advantageous characteristics but can be limiting in multicolor imaging since most ready-made fluorescent reporter constructs fluoresce in the green to red region of the visible spectrum. Nile red emits between green and red, and BODIPY can be photoconvertable from green to red fluorescent, limiting its ability to utilize it for time lapse imaging of living cells. Here, we report the design and synthesis, the photophysical characterization, and biological results with two easily prepared series of new blue fluorescing dyes as markers for LDs. Confocal fluorescence microscopy results show an interesting correlation between the chemical structure of these fluorescent probes and the specific staining pattern. The pyrazole-based structure (**6c**) is specific for LDs, whereas the pyrrole-based structure (**5d**) resulted in prominent dyeing of the membranous cell organelles.

The synthesis of fluorescent molecules has become a major research area in the last decades because, in combination with fluorescence microscopy, these compounds allow the observation or detection of living objects and their intracellular processes as well the localization and distribution of many intracellular macromolecules.[1,2] Lipid droplets (LDs) are subcellular organelles surrounded by a phospholipid monolayer containing neutral lipids, usually triacylglycerols or cholesteryl esters,[3] which for a long time were considered to be inert.[4] However, the cell biology of LDs has evolved and it is currently accepted that excessive lipid storage is associated with the pathogenesis of highly prevalent metabolic diseases such as diabetes, obesity and atherosclerosis, and may even be related to the development of certain types of cancer.[5] Despite the importance of LDs, fluorescent probes targeting them are almost restricted to BODIPY and nile red-type structures,[6a-c] although some new fluorescent structures have been developed lately for this application (Figure 1).[7a-b] However, commercially available LD dyes such as nile red and BODIPY 493/503 can be limiting in multicolor imaging, as most ready-made fluorescent reporter constructs fluoresce in the green to red region of the visible spectrum. An interesting blue-fluorescent marker for LDs is the commercially available monodansylpentane (MDH), which has been successfully used in multicolor live cell imaging supporting the importance in the discovery of new markers emitting in this region of the visible spectra.[6c]

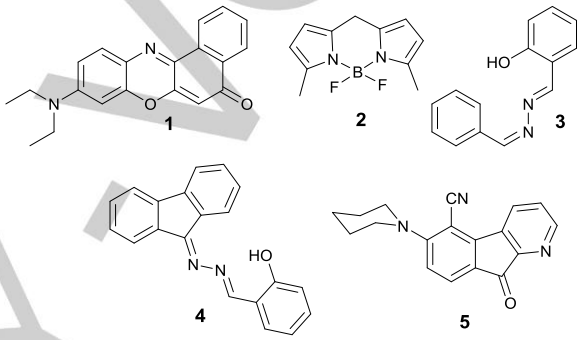

Figure 1. 1: Nile red; 2: Bodipy; 3: Azines; 4: Hydrazone-fluorenones; 5: Azafluorenones.

During the last year and as part of our ongoing research on the diastereoselective synthesis of annulated tetrahydropyridines [8] we found that 6,10-dihydrochromeno[4,3-*b*]pyrrolo[3,2-*e*]pyridine and 6,10-dihydrochromeno[4,3-*b*]pyrazolo[4,3-*e*]pyridine exhibited fluorescence. This was not surprising since the pyrazolo skeleton can be found as a subunit together with other moieties such as pyridine,[9] coumarin,[10] quinoline,[11-13] and quinoxaline,[14] in tricyclic or tetracyclic molecules that have shown fluorescent properties. The pyrrole nucleus is the essential unit in the abovementioned BODIPY fluorophores, but it has been less exploited for the synthesis of carbannulated emissive probes. Moreover, there is a rich literature regarding fluorescent molecules based on oxygen heterocyles such as benzopyran and xanthene.[15] 3-Oxo-3H-benzopyrans, commonly referred to as coumarins, and fluoresceins, eosins and rhodamines belong to each of these classes. Nevertheless, to the best of our knowledge, aza-analogues of 6H-dibenzo[b,d]pyran have not been reported in fluorescent chromophores. Thus, we decided to synthesize two series of tetracyclic pyrrolo- and pyrazolo-pyridines annulated with a dihydrochromene structure in order to study their photophysical properties and potential application as fluorescence probes. The proposed rigid structures lack any obvious possibility of internal rotation that would enhance the radiative pathway, a structural feature that has been exploited in other fluorescent probes.[16-17] All these compounds were synthesized via an intramolecular aza-Diels-Alder reaction with a slight variation of the previously reported method.[8] The first step consisted in the synthesis of aldimines **8a-d** and **9a-c** (SI). After isolation and purification, the

[a] M. Becerra-Ruiz, MSc. V. Vargas, P. Jara, CM. Carrasco, Dr. M.T. Núñez, N. Lezana, Dr. A. Galdámez, Dr. M. Vilches-Herrera
Department of Chemistry
+Department of Biology
Faculty of Sciences, University of Chile
Las Palmeras 3425, Nunoa, 7500008, Santiago (Chile)
luis.vilches@u.uchile.cl
[b] Dr. C. Tirapegui
Faculty of Chemistry and Biology, University of Santiago de Chile
Av. Lib. Bernardo O' Higgins 3363, Est. Central, Santiago, Chile
Universidad Autónoma de Chile
Supporting information for this article is given via a link at the end of the document.

final compounds **10a-c** and **11a** were obtained in a one pot procedure using propargyl bromide for alkylation and in situ cycloaddition. A well-known and widely used substituent in fluorescent probes is the diethylamino group because of its strong donor properties, which facilitate intramolecular charge transfer processes (ICT).[14, 18-19] Indeed, this photophysical phenomenon has been reported in pyrazolo[3,4-*b*]pyridine-based coumarin chromophores.[10] In that work the authors, using density functional theory (DFT), show that the electron density flows from the electron donor diethylamino group to the pyrazolopyridine core. Based on that, we envisioned that an electron withdrawing group attached to either the pyrrolo- or pyrazolopyridine core would enhance the electronic flux and consequently an ICT process. Thus, we decided to introduce an ester moiety in the pyridine ring in at least one molecule of each series to achieve two goals: on one hand to increase a possible intramolecular charge transfer and on the other to increase membrane permeability for biological evaluation.[20a-b] To this end, instead of propargyl bromide for the alkylation step we chose methyl bromocrotonate to obtain the corresponding tetrahydropyridine derivatives that were further oxidized using DDQ to obtain the final products **10d** and **11b-c**. Table 1

Table 1. Synthesis of fluorescent compounds.

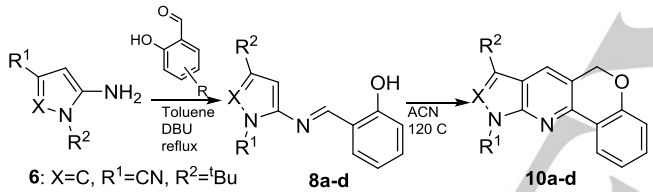

6: X=C, R^1=CN, R^2=^{t}Bu
7: X=N, R^1=CH_3, R^2=Ph

8a-d
9a-c

10a-d
11a-c

Entry	Compound	Product	Yield [%]
1	**10a**	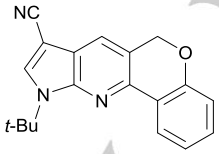	60[a]
2	**10b**	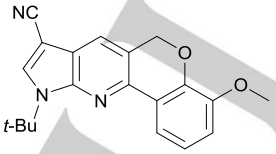	70[a]
3	**10c**	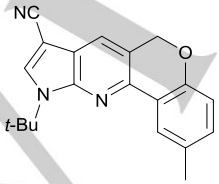	60
4	**10d**	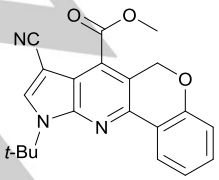	62
5	**11a**	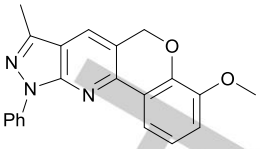	75[a]
6	**11b**	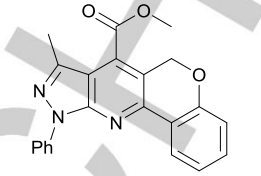	68
7	**11c**	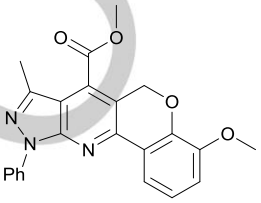	79

[a] Ref. 8

All the compounds were characterized by NMR spectroscopy. Additionally, the crystal structure of **10c** was determined by single-crystal X-ray diffraction analysis. As shown in Figure 2, the molecule is essentially planar with an average deviation from the least-squares plane of 0.0010 Å (The maximum deviation from the plane is -0.0010 Å for atom N3). In the crystal packing, molecules are linked by intermolecular π-π interactions resulting in antiparallel stacking. The perpendicular distance between the ring centroids is 3.679(4) Å with a slippage of 1.18°.

Although it is evident that the nearly planar structure of the compounds allows efficient electron delocalization between the aromatic ring of the chromane and the pyrrolo- or pyrazolopyridine core, we synthesized a derivative of **10a (10a`)**, where the oxygen-carbon bond of the pyran ring was broken. Along with its NMR characterization, its structure was confirmed by single-crystal X-ray diffraction analysis. Here the phenyl ring is twisted with respect to the pyrrolopyridine skeleton forming a dihedral angle of 58.6°. As we expected, the fluorescence properties disappeared with the rigidity of the molecule, highlighting the role of the electron-intercommunication in the emissive properties of the compounds.

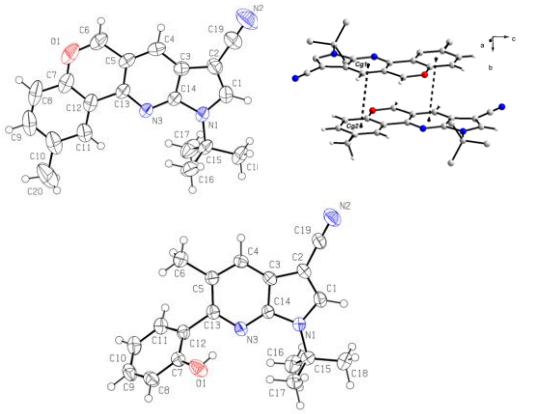

Figure 2. The molecular structure of **10c** (up, CCDC 1570750) and **10a´**(down, CCDC 1570749). Displacement ellipsoids are drawn at the 50% probability level. (right) A part of the crystal structure showing the formation of π-π interactions (dashed lines). Cg1 and Cg2 are the centroids of the pyridine and benzene rings, respectively, and are denoted by small spheres.

The solvatochromic behavior of all the synthesized compounds was investigated in a series of solvents with different polarity indexes. For all of them, the absorption spectra were nearly independent of solvent polarity (S4). However, in the fluorescence spectra, bathochromic shifts were observed with increasing polarity, indicating a greater dipole moment in the excited state than in the ground state of the molecule. This feature is typical of molecules that undergo an intramolecular charge transfer (ICT) process and is normally associated with positive solvatochromism.[7a, 10] (SI) Stokes shifts, molar extinction coefficients (ε) and quantum yields (ϕ) measured in $CHCl_3$ and EtOH are presented in Table 2.

Table 2. Spectroscopic data of the synthesized compounds.

Product	Φ_f EtOH	Φ_f $CHCl_3$	ε, $mol^{-1}L\ cm^{-1}$	ε, $mol^{-1}L\ cm^{-1}$	Stokes shift nm $CHCl_3$	Stokes shift nm EtOH
10a	0,543	0,691	15317	22000	2557	2740
10b	0,147	0,280	8932	12600	4396	4700
10c	0,005	0,036	14020	14500	3985	3920
10d	0,183	0,322	12353	12400	5818	6776
11a	0,061	0,093	17301	11700	6079	6297
11b	0,328	0,597	13993	20500	7881	9178
11c	0,003	0,029	11272	13200	8875	10031

From the plot of the excitation wavelengths versus the empirical polarity parameters ET(30) [22] of the solvents, it can be seen that the magnitude of the Stokes shift values increases as a function of solvent polarity on going from heptane to methanol. Interestingly, compounds **11a-c** show higher values compared with compounds **10a-d**. This observation implies a greater difference between the excited states reached by the pyrazolopyridine series after absorption and those from which the emission starts, than for the pyrrolopyridine series.[21]

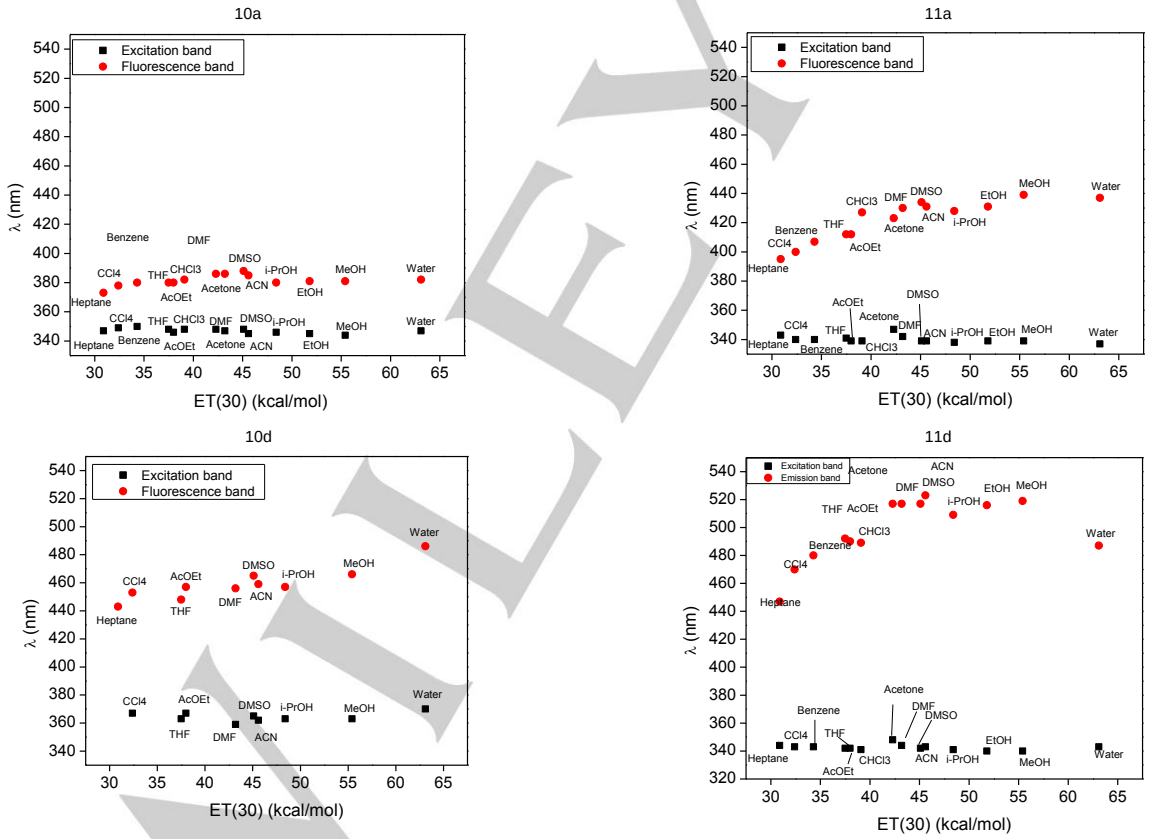

Figure 3. Plot of the excitation wavelengths v/s ET(30) of the solvents for the compounds **10a**, **10d**, **11a** and **11c** .

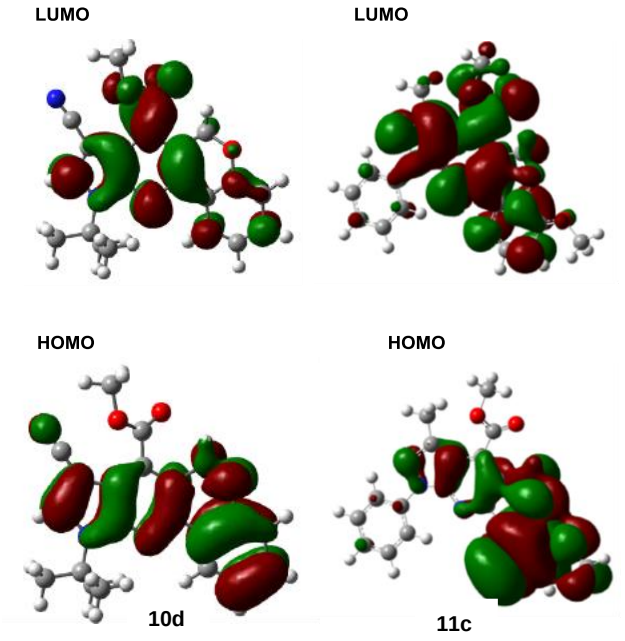

Figure 4. Calculated molecular orbitals HOMOs and LUMOs of compounds **10d** and **11c**.

From this plot, it can be also seen that, for each series, the magnitude of the Stokes shift values increases with the number of substituents. Thus, **10d** and **11c** showed higher values in comparison with **10a** and **11a** respectively (Figure 3). All the compounds exhibit intense blue fluorescence, although lower quantum yields were obtained in ethanol than in chloroform, which is attributable to the so-called positive solvatokinetic effect. This behavior is usually found in molecules with ICT character due to the strong interaction between the solvent and the polarized molecule in the excited state.[23] As the lower ϕf was measured in a protic solvent, hydrogen bond interactions between the molecule and the surrounding solvent can be present resulting in additional non-radiative decay.[9] In contrast with the Stokes shift values, the addition of a substituent probably decreased the ϕf because of the modulation of the radiative versus the non-radiative pathway upon introduction of more substituents. The highest value was observed for **10a**. Additionally, considering that substituents that enhance electron mobility will increase the fluorescence intensity, it can be affirmed that an electron withdrawing group such as ester is more effective that an electron donor group such as methoxy. Thus, **10d** and **11b** showed higher ϕf in comparison with **10b** and **11a** respectively. It is, however unclear the decay in the ϕf of **10c** versus **10a** due the incorporation of a methyl group and the lower ϕf of **11c**.

Electronic and geometric properties of all the compounds were investigated using a B3LYP/6-31G method with the Gaussian G-09 program.[24] The geometry optimizations are consistent with the planarity observed in the single crystal structure. The molecular orbitals of all the compounds are shown in Figure 4, and SI. The electron density in terms of HOMO and LUMO are dependent of the substitution pattern. With a methoxy group the electronic distribution is strongly localized in the aromatic ring of the chromane. Such is the case of **10b** and **11c** and to a lesser extent **11a**, but also with a weaker donor like a methyl group in **10c**. In general, however, after excitation, an electron delocalization between the annulated aromatic ring (HOMO) and the bicyclic heteroaromatic core (LUMO) is seen. This can be described as an intramolecular π-π* charge-transfer transition, from the benzene ring to a similar orbital of the heterobiaryl ring. Although the orbital coefficient in the LUMO of **10d** is only slightly higher than in **10a**, the introduction of an ester moiety in the pyridine ring seems to enhance the ICT process. In case of compounds **11a** and **11c**, the calculated HOMO is localized on different parts of the molecule as consequence of the additional methoxy group. However, in all cases the calculated LUMO is localized on the ester group supporting our original idea. Electronic transitions, the energy band gap and oscillator strength corresponding to HOMO→LUMO and HOMO-1 → LUMO, were calculated for all compounds (SI).

To investigate the potential application of these compounds as fluorescence probes, we tested them for bioimaging in SH-SY5Y human neuroblastoma cells. A preliminary assay using epifluorescence microscopy was carried out to evaluate the capacity of the compounds to stain the cells. Interesting, from the comparison between ester-free and ester-containing dyes, it was evident that the ester group play an important role on the cellular uptake as we predicted. **10d** and **11c** showed higher fluorescence than **10a** and **11a** respectively. Moreover, **11c** was used at a concentration of 1 μM whereas all the other compounds were evaluated at 10 μM (SI). Based on this analysis we further assessed the capability of compounds, **10d** and **11c** to enter and stain the cytosol using fluorescence confocal microscopy. To our delight, these results showed a specific pattern of staining on spherical organelles that we identified as lipid droplets (LDs). To confirm our assumption, we performed an additional experiment of co-localization with nile red which is a well-known LD marker. From this experiment, and as shown in Figure 5, we can highlight two interesting observations. On one hand, **11c** proved to be very selective for LDs comparable with the commercially marker. On the other hand, **10c** and **10d** showed a marked preference for LDs but also presented a cytoplasmatic distribution and **10d** had a high preference for membranes, making it possible to identify easily the plasma and nuclear membrane. Indeed, these bright blue fluorescence probes might easily be used in combination with other green and red fluorescent reporters for multicolor fluorescence imaging such as with MDH, previously mentioned. A comparison between our series and this or other blue fluorescent markers would be highly desirable but is not the goal of this article. Envisioning the use of these compounds in live cell imaging, cytotoxicity evaluation was performed showing a good cell viability up to 100 μM concentration (SI).

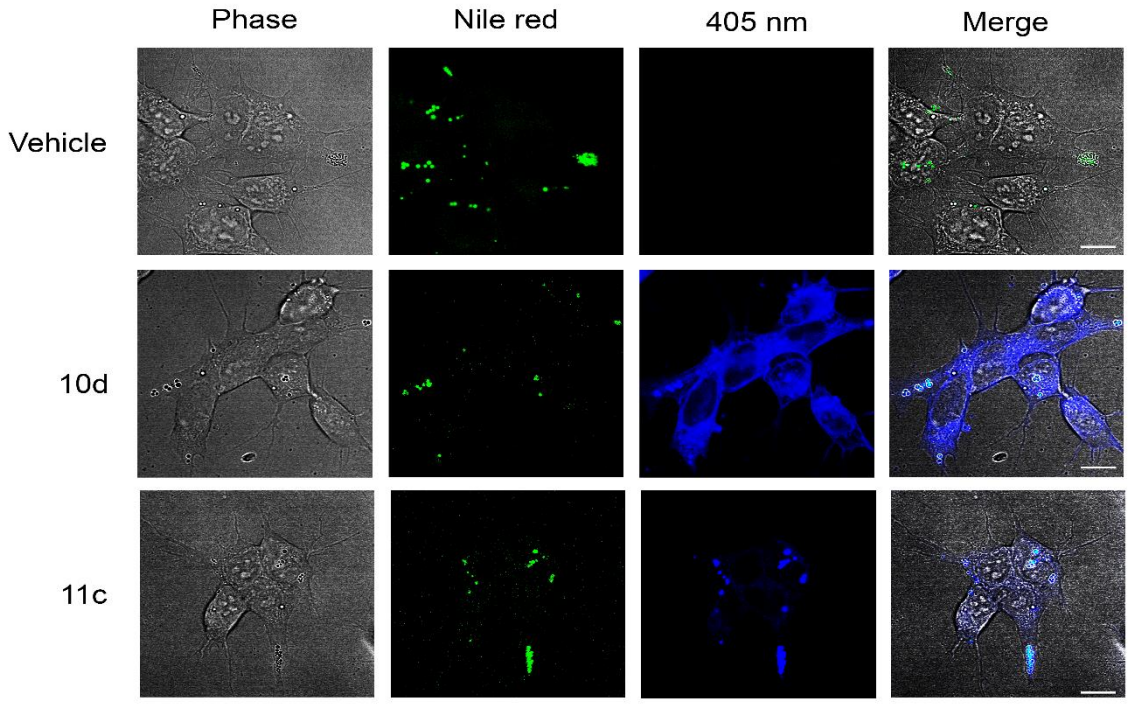

Figure 5. Confocal fluorescence microscopy images of compounds **10d**, **11c** and nile red in SH-SY5Y human neuroblastoma cells.

Conclusions

Two new series of 6,10-dihydrochromeno[4,3-*b*]pyrrolo[3,2-*e*]pyridine and 6,10-dihydrochromeno[4,3-*b*]pyrazolo[4,3-*e*]pyridine derivatives were synthesized. The photophysical properties and potential application of these compounds as fluorescent probes were evaluated. According to the solvatochromic behaviour and photophysical calculations, an intramolecular charge transfer process was established for both series. This process would depend on the number and placement of the substituents and their electron distribution in ground and excited states and the respective FMO delocalization. The introduction of an ester moiety in the pyridine ring correlates with the compounds' strong response in the fluorescence assay, probably because of their enhanced membrane permeability. Compound **11c** is a novel specific dye for lipid droplets (LDs) comparable with nile red, and **10d** is useful for cell membrane staining. Considering that **11c** is pyrazole-based and **10d** are pyrrole-based structures, their dissimilar response toward the biological target is a valuable clue for the design of new specific fluorescent probes based on aminoheterocycles, which is part of our current investigation.

Experimental Section

General procedure for compounds **8a-d** and **9a-c**: 1-(tert-butyl)-1H-pyrrole-3-carbonitrile (500mg, 3.06mmol, 1eq) and corresponding 2-hydroxy-benzaldehyde (3.06mmol, 1eq) was added to methanol (30ml). After refluxed the mixture over 6h with magnetic stirring, the solution was cooled to 0°C in an ice/water bath until precipitation. Yellow crystals were obtained by filtration under vacuum conditions; Compound **8c**: 1-(tert-butyl)-1H-pyrrole-3-carbonitrile (500mg, 3.06mmol, 1eq), 2-hydroxy-5-methylbenzaldehyde (418mg, 3.06mmol, 1eq), DBU (0.46ml, 3.06mmol, 1eq) was added to toluene (5ml) under nitrogen atmosphere in a pressure tube. The mixture was warmed at 160°C for 6h with magnetic stirring. After removal of the toluene by vacuum distillation, ethyl acetate (35ml) and water (30ml) with five drops of fuming HCl was added and the solution was extracted. The layer was separated and the aqueous layer was extracted by ethyl acetate (4 x 12mL). The organic layer was combined, dried over anhydrous magnesium sulfate, filtered and evaporated in vacuo. Methanol (15mL) was added to the slurry and the solution was cooled to 0°C in an ice/water bath until precipitation. Yellow crystals were obtained by filtration under vacuum conditions.

General Procedure for compounds **8d** and **10b-c**: the corresponding imine (3.74mmol, 1eq), methyl 4-bromocrotonate (0.65mL, 5.82mmol, 1.5eq) and potassium carbonate (2.58g, 5eq) was added to acetonitrile (40mL). The mixture was refluxed for 8h with magnetic stirring. After cooling, the solvent was evaporated, and the residue was dissolved in ethyl acetate (15mL). Water (15mL) was added and the mixture stirred for 15 min at room temperature. The organic phase was separated,

and the aqueous layer was extracted with ethyl acetate (3x12mL). The combined organic phases were dried over anhydrous sodium sulfate, filtered and concentrated under reduce pressure, dissolved in 15mL of methanol or in a mixture of hexane/ethyl acetate (4:1, 15mL) for crystallization and left overnight. The formed crystals were filtered to give the corresponding products. No other purification method was used (e.g column chromatography); Compounds **10a-c** and **11a**: The corresponding imine (3.74mmol, 1eq), propargyl bromide (80 wt. % in toluene) (0.65mL, 5.82mmol, 1.5eq) and potassium carbonate (2.58g, 5eq) were refluxed in 40 ml of acetonitrile for 8h with magnetic stirring. After cooling, the solvent was evaporated, and the residue was dissolved in ethyl acetate (15mL). Water (15mL) was added and the mixture stirred for 15 min at room temperature. The organic phase was separated, and the aqueous layer was extracted with ethyl acetate (3x12mL). The combined organic phases were dried over anhydrous sodium sulfate, filtered and concentrated under reduce pressure to give a solid material that was used for the next step without further purification. The solid and p-xylene (10mL) was added into a pressure tube and heated at 120°C for 6h with magnetic stirring. After removal of the solvent by vacuum distillation, methanol (10ml) was added. The solution was cooled to 0°C in a ice/water bath until precipitation. Crystals were filtrated and dried at room temperature; compounds **10d** and **11b-c**: the corresponding tetrahydropyridine (1.78mmol, 1eq) and DDQ (1.212g, 5.34mmol, 3eq) was stirred in acetonitrile (45 mL) at room temperature for 3h. Afterwards, the mixture was filtered and the solid was crystallized in methanol (50ml).

(1-(tert-butil)-6-(2-hidroxifenil)-1H-pirrol[2,3-b]piridina-3-carbonitrilo) **10a`**: Yield: 60%. 1H-NMR (400MHz, CDCl3) δ = 10.17 (s, 1H), 8.06 (s, 1H), 7.88 (s, 1H), 7.50 (dd, J = 7.8, 1.3Hz, 1H), 7.32 (m, 1H), 7.09 (d, J = 8.2Hz, 1H), 6.98 (m, 1H), 2.60 (s, 3H), 1.82 (s, 9H).

10-(tert-butil)-2-metil-6,10-dihidrocromeno[4,3-b]pirrol[3,2-e]piridina-8-carbonitrilo **10c:** Yield: 60%. Decomposition temperature: 261°C. 1H-NMR (400MHz, CDCl3) δ = 8.02 (s, 1H), 7.82 (s, 1H), 7.76 (s, 1H), 7.13 (d, J = 8.2Hz, 1H), 6.90 (d, J = 8.2Hz, 1H), 5.28 (s, 2H), 2.41 (s, 3H), 1.89 (s, 9H). 13C-NMR (400MHz, CDCl3) δ = 154.47, 147.02, 144.11, 133.02, 131.72, 131.48, 124.63, 123.56, 123.24, 121.31, 120.26, 116.84, 115.42, 83.26, 68.48, 58.53, 29.16, 26.84, 20.89.

(10-(tert-butil)-8-ciano-6,10-dihidrocromeno[4,3-b]pirrol[3,2-e]piridina-7-carboxilato) **10d**: Yield: 62%. mp: 211-213°C. 1H-NMR (400MHz, CDCl3) δ = 8.23 (d, J = 7.7Hz, 1H), 7.97 (s, 1H), 7.34 (t, J = 7.5, 7.8Hz, 1H), 7.12 (t, J = 7.4Hz, 1H), 7.00 (d, J = 8.1Hz, 1H), 5.56 (s, 2H), 4.10 (s, 3H), 1.89 (s, 9H). 13C-NMR (400MHz, CDCl3) δ = 165.66, 157.02, 147.91, 144.87, 136.66, 131.89, 128.23, 125.27, 123.51, 122.76, 121.82, 117.52, 116.91, 116.31, 84.81, 66.82, 59.48, 52.34, 29.65.

methyl 4-methoxy-8-methyl-10-phenyl-6,10-dihydrochromeno[4,3-b]pyrazolo[4,3-e]pyridine-7-carboxylate **11c**: Yield: 79%. mp: 166-167°C. 1H-NMR (400MHz, CDCl3) δ = 8.32 (d, J = 8.1Hz, 2H), 7.93 (d, J = 7.9Hz, 1H), 7.53 (t, J = 7.8, 7.6Hz, 2H), 7.31 (t, J = 7.2, 7.3Hz, 1H), 7.08 (t, J = 8.0, 7.9Hz, 1H), 6.98 (d, J = 8.0Hz, 1H), 5.44 (s, 2H), 4.06 (s, 3H), 3.92 (s, 3H), 2.58 (s, 3H). 13C-NMR (400MHz, CDCl3) δ = 165.59, 150.89, 149.01, 148.68, 146.69, 142.00, 139.29, 130.29, 129.00, 125.76, 123.66, 122.06, 121.00, 118.83, 117.50, 114.10, 111.81, 66.82, 56.21, 52.74, 14.54.

Spectral data for compounds **10a-b** and **11a** was according to the literature.[8]

Acknowledgements

We acknowledge financial support by FONDECYT Grant Number 11160465 and VID Grant UI003/16

Keywords: Lipid droplets • Blue fluorescent probes • aza-Diels-Alder reaction • aminoheterocycles • confocal fluorescence microscopy

[1] T. Ueno and T. Nagano, *Nature Methods* **2011**, 8, 642-645.
[2] T. Terai and T. Nagano, *Curr. Opin. Chem. Biol.* **2008**, 12, 515–521; M. Terasaki, L. Loew, J. Lippincott-Schwartz, K. Zaal, *Curr. Protoc. Cell Biol.*, **1998**, 4.4.1-4.4.18.
[3] S. Martin, R. G. Parton, *Cell Dev. Biol*. **2005**,16, 163–174.
[4] T. Fujimoto, R. G. Parton, *Cold Spring Harb Perspect Biol* **2011**; 3:a004838.
[5] Y. Guo, K. R. Cordes, R. V. Farese, T. C. Walthe r, *J. Cell Sci.* **2009**,122, 749-752.
[6] a) P. Greenspan, E. Mayer, S. Fowler, *J. Cell Biol***. 1985**, 100, 965−973; b) E. E., Spangenburg, S. J. P. Pratt, L. M Wohlers, R. M. Lovering. *J. Biomed. Biotechnol*. **2011**, 598358; c) H.J. Yang, Ch.L. Hsu, J.Y. Yang, W.Y. Yang, *PLoS One*. **2012**, 7(3): e32693
[7] a) A. Sharma, S. Umar, P. Kar, K. Singh, M. Sachdev, A. Goel, *Analyst*, **2016**, 141, 137–143; b) Z. Wang, C. Gui, E. Zhao, J. Wang, X. Li, A. Qin, Z. Zhao, Z. Yu, B. Zhong Tang*, ACS Appl. Mater. Interfaces* **2016**, 8, 10193−10200.
[8] N. Lezana, M. Matus-Pérez, A. Galdámez, S. Lühr, M. Vilches-Herrera, *Green Chem.*, **2016**, 18, 3712–3717.
[9] B. Varghese, S.N. Al-Busafi, F.E.O. Suliman, S. M.Z. Al-Kindy, *JOL.* **2015**, 159, 9 –16.
[10] J. Chen, W. Liu, J. Ma, H. Xu, J. Wu, X. Tang, Z. Fan, P. Wang, *J. Org. Chem*. **2012**, 77, 3475−3482.
[11] M. Mac, T. Uchacz, T. Wróbel, A. Danel, E. Kulig, *J. Fluoresc.* **2010**, 20, 525–532.
[12] M. Mac, T. Uchacz, A. Danel, K. Danel, P. Kolek, E. Kulig, *J. Fluoresc*. **2011**, 1, 375–383.
[13] K. Rurack, A. Danel, K. Rotkiewicz, D. Grabka, M. Spieles, W. Rettig, *Org. Lett.* **2002**, 4, 4647-4650.
[14] P. Wang, Z. Xie, Z. Hong, J. Tang, O. Wong, C.S. Lee, N. Wong, S. Lee, *J. Mater. Chem*., **2003**, 13, 1894–1899.
[15] M. Sameiro T. Gonçalves, *Chem. Rev*. **2009**, 109, 190–212.
[16] F. Kohl, J. Schmitz, N. Furtmann, A.-C. Schulz-Fincke, M. D. Mertens, J. Kuppers, M. Benkhoff, E. Tobiasch, U. Bartz, J. Bajorath, M. Stirnberg, M. Gutschow, *Org. Biomol. Chem.* **2015**, 13, 10310.
[17] L. Wang, C.W. Barth, M. Sibrian-Vazquez, J.O. Escobedo, M. Lowry, J. Muschler, H. Li, S. L Gibbs, R. M. Strongin, *ACS Omega* **2017**, 2, 154.
[18] P. Wang, S. Wu, *J. Photochem. Photobiol. A: Chem*. **1995**, 86, 109-113
[19] O. García-Beltrán, N. Mena, O. Yañez, J. Caballero, V. Vargas, M. T. Nuñez, B. K. Cassels, *Eur. J. Med. Chem*. **2013**, 67, 60-63.
[20] a) K. Beaumont, R. Webster, I. Gardner, K. Dack, *Curr. Drug Metab*. **2003**, 4(6), 461-485; b) J. Rautio, H. Kumpulainen, T. Heimbach, R. Oliyai, D. Oh, T. Järvinen, J. Savolainen, *Nat. Rev. Drug Discov.* **2008**, 7(3), 255-270.
[21] C. Du, J. Chen, Y. Guo, K. Lu, S. Ye, J. Zheng, Y. Liu, Z. Shuai, G. Yu, *J. Org. Chem.* **2009**, 74, 7322-7327.

[22] C. Reichardt*, Chem. Rev*. **1994**, 94, 2319 - 2358.

[23] P. Wang, Z. Xie, Z. Hong, J. Tang, O. Wong, CS. Lee, N. Wong, S. Lee, *J. Mater. Chem.* **2003**, 13, 1894-1899.

[24] M. J. Frisch, G. W. Trucks, H. B. Schlegel, G. E. Scuseria, M. A. Robb, J. R. Cheeseman, G. Scalmani, V. Barone, B. Mennucci, G. A. Petersson, H. Nakatsuji, M. Caricato, X. Li, H. P. Hratchian, A. F. Izmaylov, J. Bloino, G. Zheng, J. L. Sonnenberg, M. Hada, M. Ehara, K. Toyota, R. Fukuda, J. Hasegawa, M. Ishida, T. Nakajima, Y. Honda, O. Kitao, H. Nakai, T. Vreven, J. A. Montgomery Jr., J. E. Peralta, F. Ogliaro, M. Bearpark, J. J. Heyd, E. Brothers, K. N. Kudin, V. N. Staroverov, T. Keith, R. Kobayashi, J. Normand, K. Raghavachari, A. Rendell, C. Burant, S. S. Iyengar, J. Tomasi, M. Cossi, N. Rega, J. M. Millam, M. Klene, J. E. Knox, J. B. Cross, V. Bakken, C. Adamo, J. Jaramillo, R. Gomperts, R. E. Stratmann, O. Yazyev, A. J. Austin, R. Cammi, C. Pomelli, J. W. Ochterski, R. L. Martin, K. Morokuma, V. G. Zakrzewski, G. A. Voth, P. Salvador, J. J. Dannenberg, S. Dapprich, A. D. Daniels, O. Farkas, J. B. Foresman, J. V. Ortiz, J. Cioslowski and D. J. Fox, Gaussian 09 (Revision D.01), Gaussian, Inc., Wallingford CT, 2013.

10.1002/ejoc.201701633

WILEY-VCH

Entry for the Table of Contents (Please choose one layout)

Layout 1:

FULL PAPER

Fluorescent probes allow the observation, detection or distribution of living objects in the intracellular space. Because of lipid storage is associated with the pathogenesis of highly prevalent metabolic diseases the detection of lipid droplets, a type of subcellular organelle is important. Herein, the synthesis of two series of blue fluorescent probes is reported.

*M. Becerra-Ruiz,V. Vargas, P. Jara, C. Tirapegui, CM. Carrasco, M.T. Nuñez, N. Lezana, A. Galdámez, and M. Vilches-Hererra**

Blue-fluorescent probes for lipid droplets based on dihydrochromeno-pyrazolepyridine and pyrrolopyridine